Analyses of shock waves and jams in traffic flow

2005 J. Phys. A: Math. Gen. 38 4069

(http://iopscience.iop.org/0305-4470/38/19/002)

INSTITUTE OF PHYSICS PUBLISHING JOURNAL OF PHYSICS A: MATHEMATICAL AND GENERAL

J. Phys. A: Math. Gen. **38** (2005) 4069–4083 doi:10.1088/0305-4470/38/19/002

Analyses of shock waves and jams in traffic flow

A K Gupta and V K Katiyar

Department of Mathematics, Indian Institute of Technology Roorkee, Roorkee 247 667, India

E-mail: arvindma@iitr.ernet.in and vktmafma@iitr.ernet.in

Received 25 October 2004, in final form 9 March 2005
Published 25 April 2005
Online at stacks.iop.org/JPhysA/38/4069

Abstract

In this paper, we study the certain qualitative properties of a new anisotropic continuum traffic flow model in which the dimensionless parameter or anisotropic factor controls the non-isotropic character and diffusive influence. We discussed the travelling wave solution for our model and find out the condition for the shock wave. Shock and rarefaction waves are obtained from the new model and are consistent with the diverse nonlinear dynamical phenomena observed in a real traffic flow. However, our model for large values of anisotropic parameter removes the discontinuity as pointed out by Berg *et al* (2000 *Phys. Rev.* E **61** 1056). The nonlinear theory of the cluster effect in a traffic flow i.e., the effect of appearance of a region of high density and low average velocity of vehicles in an initially homogeneous flow, is also discussed. It is shown that an appearance of a localized perturbation of finite amplitude in the stable homogeneous flow can lead to a self-formation of a local cluster of vehicles. It is also been observed that the cluster effect from our model shows a good agreement with the results of Kerner and Konhäuser (1994 *Phys. Rev.* E **50** 54) and Jiang *et al* (2002 *Trans. Res.* B **36** 405).

PACS numbers: 46.05.+b, 45.70.Vn

(Some figures in this article are in colour only in the electronic version)

1. Introduction

Traffic flow models are used to analyse and predict traffic flow on road networks. Recently, considerable attention has been paid to traffic flow problems [1, 2]. Apart from experimental observations, Gerlough *et al* [3] and Helbing [4] proposed physical models of traffic flow situations. Continuum models give an overview of the global traffic flow, which is needed for understanding the collective behaviour of traffic and designing efficient control strategies, and allow analytical validations. Fundamentals of traffic flow modelling and control are the basic relationship between three traffic states: flow rate (q), mean velocity (v) and vehicle density (ρ).

Since the seminal work by Lighthill and Whitham [5] and Prigogine [7] on kinetic theory of traffic flow, vehicles have often been considered as interacting particles and traffic flow can be considered as a one-dimensional compressible flow of these particles. Due to analogies with gas theory [8] and fluid dynamics [5, 7, 9–15], modelling and simulating traffic flow increasingly attracts the attention of physicists and engineers. The study of continuum models began with the LWR model developed independently by Lighthill and Whitham [5] and Richards [6]. The LWR model is known as the simple continuum model in which the relationships among three aggregate variables (ρ, v and q) are modelled. The LWR model employs the conservation equation in the following form:

$$\frac{\partial \rho}{\partial t} + \frac{\partial q}{\partial x} = 0. \tag{1}$$

Equation (1) is not a self-consistent model but needs an additional relation which is supplemented by the following equation of traffic flow,

$$q = \rho v, \tag{2}$$

and a relationship between the mean velocity and the traffic density under steady-state uniform flow

$$v = v_e(\rho), \tag{3}$$

where $v_e(\rho)$ is the equilibrium velocity; x and t represent space and time respectively.

The waves described by the simple continuum model are kinematic waves in the sense that no dynamic law is used in the model. It is simple yet sufficiently powerful to describe the most basic traffic flow phenomena such as traffic congestion formation and dissipation in dense traffic. The consistency and existence of weak solutions of such conservation laws have been studied by Zhang [16] and Lax [17] respectively.

Although the LWR model makes sensible predictions of propagation and dissipation of traffic jams, it fails to model two important traffic phenomena: the stop–start wave caused by instability in traffic flow and forward propagation of disturbances in heavy traffic.

In the past decades, many efforts were devoted to improving the LWR model through developing higher order models, which use a dynamic equation for the speed (v) to replace the equilibrium relationship (3). Perhaps the most well-known result of these efforts is the higher order model developed by Payne [9]. In the Payne model, the fluctuation of speed around the equilibrium values is allowed; thus, the model is suitable for the description of non-equilibrium situations such as stop-and-go traffic etc. Payne uses a dynamic equation for the mean velocity v to replace the equilibrium relationship (3). The dynamic equation of Payne's model is derived from car-following theory and has the following form:

$$\frac{\partial v}{\partial t} + v\frac{\partial v}{\partial x} = \frac{v_e(\rho) - v}{T} + \frac{v_e'(\rho)}{2\rho T}\frac{\partial \rho}{\partial x}, \tag{4}$$

where T is the relaxation time and $v_e'(\rho) = \frac{\mathrm{d}v_e(\rho)}{\mathrm{d}\rho}$.

Over the past four decades, velocity–density relation (equilibrium function) has been the subject of intensive research. There are two approaches for stating the equilibrium function: (i) the classical approach and (ii) the phenomenological approach. The classical approach is a purely mathematical one and the phenomenological approach is based on assumptions about the driver's behaviour with respect to some traffic variables.

Later, several authors [10–12] suggested a considerable number of modifications to Payne's model. However, as pointed out by Daganzo [18], it was shown that the Payne model [9] and the other listed non-equilibrium models [10–12] have two families of characteristic, along which traffic information is transmitted: one is slower and the other is faster than the speed

of the traffic stream that carries them. The faster characteristic leads to a gas-like behaviour (vehicles from behind can force vehicles in front to speed up) [19], and diffusion causes 'wrong way' travel [18]. One fundamental principle of the traffic flow is that vehicles are anisotropic and respond only to the frontal stimuli. Recently, Zhang [13, 14] proposed new non-equilibrium models and showed that the new models overcome the backward travel problem. But different from the LWR model, the Payne-type model (higher order models) can be unstable due to the non-uniformity of the traffic flow. Whitham [20] finds out the stability condition for the linearized system with a relaxation term. When the Payne-type models are unstable, Kerner and Konhäuser [21] observed cluster solution. Recently, some authors [22, 23] have brought about an interesting improvement in the modelling of traffic flow by a hydrodynamic equation. Coscia [22] developed a mathematical model for the closure of mass conservation equation. Bürger and Karlsen [23] extended the LWR model in order to include both abruptly changing road surface conditions and driver's reaction time and anticipation length.

The problem of traffic congestion is becoming endemic due to increased levels of populations owning automobiles. The increased number of vehicles on roads causes intervention in the free movement of traffic and interruption in driving according to one's own intention. Traffic congestion in an initially homogeneous traffic flow can be explained by a cluster effect in a traffic flow [11]. In a real traffic flow almost every driver moving on a long road occasionally meets with the phenomenon of traffic congestion. Kerner and Konhäuser [11] have recently confirmed the phenomenon of 'phantom traffic jam' by the investigations of the local cluster effect: a self-formation of a local cluster of vehicles in the initially homogeneous traffic flow. Indeed, it has been found that, if the density of vehicles exceeds some critical value, the initially homogeneous traffic flow loses its stability with respect to a growth of a long wavelength non-homogeneous perturbation. Herrmann and Kerner [24] discussed in detail the local cluster effect. But in discussing the local cluster effect, Kerner and Konhäuser [11], in their one-dimensional compressible flow model take the viscosity and variance of velocity distribution as a constant. Jiang *et al* [25] developed a new anisotropic model and discussed the local cluster effect. He has taken the disturbance propagation speed as a constant. But in real situations all these parameters depend on the traffic density [12–15, 29]. Recently, some scientists [26–28] investigated the spatial–temporal real feature of traffic flow phase: free flow, synchronized flow and wide moving jam.

In this paper, we develop a new macroscopic continuum model by introducing a new speed gradient term as the anticipation term in the equation of motion. It will solve the characteristic speed problem that exists in the previously developed high-order models [10–12] and therefore can describe the traffic flow dynamics more realistically.

In section 2, we present an improved continuum model based upon the car-following model given by Jiang *et al* [25] and using the series expansion between headway and density given by Berg *et al* [15] and discussed some qualitative properties including stability analysis of the new model. In sections 3 and 4, we study the travelling wave solution and numerical scheme of the model respectively. We then analyse the shock waves and rarefaction waves in section 5 and the local cluster effect in section 6. Finally, in section 7, we provide a discussion on our results.

2. The model and its mathematical properties

2.1. A new continuum model

The car-following model was developed to model the motion of vehicles following each other on a single lane without overtaking. Car-following models present the only class of

models that describes each vehicle in a deterministic manner including the response to local variables such as speed, headway and change of headway. Therefore they seem to be of great importance with regard to autonomous cruise control systems, which should stabilize the flow and maximize the flow rate. In this paper, we follow Jiang's model [25] of road traffic, in which the acceleration of every vehicle is determined by

$$\frac{\mathrm{d}v_n(t)}{\mathrm{d}t} = a[V_e(b_n) - v_n(t)] + \alpha\lambda\Delta v \tag{5}$$

where $\Delta v = v_{n-1}(t) - v_n(t)$, with v_{n-1} and v_n being the speed of leading and following car respectively, V_e is the optimal velocity function, b_n is the headway and a is the driver's sensitivity which equals the inverse of the driver's reaction time.

It is generally believed that the headway can be written as a perturbation series [15]. Inserting the approximate expression about headway into equation (5), we can easily obtain the traffic flow dynamics equation. The full description of this new non-equilibrium theory is given by a system of partial differential equations with the first being the vehicle conservation and the second speed dynamics,

$$\frac{\partial\rho}{\partial t} + \frac{\partial(\rho v)}{\partial x} = 0 \tag{6}$$

$$\frac{\partial v}{\partial t} + v\frac{\partial v}{\partial x} = a[\overline{V}(\rho) - v] + a\overline{V}'(\rho)\left[\frac{1}{2\rho}\frac{\partial\rho}{\partial x} + \frac{1}{6\rho^2}\frac{\partial^2\rho}{\partial x^2} - \frac{1}{2\rho^3}\left(\frac{\partial\rho}{\partial x}\right)^2\right] - 2\beta c(\rho)\frac{\partial v}{\partial x}, \tag{7}$$

where $\overline{V}'(\rho) = \frac{\mathrm{d}\overline{V}(\rho)}{\mathrm{d}\rho}$, β is a non-negative dimensionless parameter and $c(\rho) < 0$ is the traffic sound speed given by

$$c^2(\rho) = -\frac{a\overline{V}'(\rho)}{2}. \tag{8}$$

Note that if $\beta = 0$, then the model reduces to Berg's model [15] and after leaving the term of $\left(\frac{\partial\rho}{\partial x}\right)^2$, it converts into the model given by Zhou *et al* [29]. Equation (7) is analogous to the Zhang model [13]. However, an important difference between that model and the new model lies in the coefficient of higher order terms.

2.2. Qualitative properties of the model

The system (6), (7) has a similar structure to Berg's model [15] and Zhou's models [29] but is more general than these models. On comparing, we get that our model has an additional term $2\beta c(\rho)\frac{\partial v}{\partial x}$. Moreover, the term $c(\rho)$ varies with OV function. These differences, however, are not the structural differences. So one would expect that the new model behaves roughly the same as Berg's and Zhou's models and perhaps gives a more accurate description of traffic flow owing to its greater generality.

We rewrite the system (6), (7) as follows:

$$\begin{pmatrix}\rho\\ v\end{pmatrix}_t + \begin{pmatrix} v & \rho \\ \frac{-a\overline{V}'(\rho)}{2\rho} & v + 2\beta c(\rho)\end{pmatrix}\begin{pmatrix}\rho\\ v\end{pmatrix}_x = \begin{pmatrix} 0 \\ a(\overline{V}(\rho) - v) + a\overline{V}'\left(\frac{1}{6\rho^2}\frac{\partial^2\rho}{\partial x^2} - \frac{1}{2\rho^3}\left(\frac{\partial\rho}{\partial x}\right)^2\right)\end{pmatrix}. \tag{9}$$

The corresponding homogeneous inviscid system of (9) can be written as

$$\begin{pmatrix}\rho\\ v\end{pmatrix}_t + \begin{pmatrix} v & \rho \\ \frac{-a\overline{V}'(\rho)}{2\rho} & v + 2\beta c(\rho)\end{pmatrix}\begin{pmatrix}\rho\\ v\end{pmatrix}_x = 0, \tag{10}$$

or $\frac{\partial U}{\partial t} + [A]\frac{\partial U}{\partial x} = 0$ is strictly hyperbolic, with eigenvalues $\lambda_1 < \lambda_2$,

$$\lambda_{1,2} = v + \left(\beta \pm \sqrt{1+\beta^2}\right)c(\rho) \tag{11}$$

and right eigenvectors

$$r_1(\rho, v) = \left(1, \left(\beta + \sqrt{1+\beta^2}\right)\frac{c(\rho)}{\rho}\right)^t, \tag{12}$$

$$r_2(\rho, v) = \left(1, \left(\beta - \sqrt{1+\beta^2}\right)\frac{c(\rho)}{\rho}\right)^t. \tag{13}$$

Moreover, the two characteristic fields of (10) corresponding to the right eigenvectors are genuinely nonlinear,

$$\nabla\lambda_1(\rho, v)r_1(\rho, v) = \left(\beta + \sqrt{1+\beta^2}\right)\left(c'(\rho) + \frac{c(\rho)}{\rho}\right) < 0 \tag{14}$$

$$\nabla\lambda_2(\rho, v)r_2(\rho, v) = \left(\beta - \sqrt{1+\beta^2}\right)\left(c'(\rho) + \frac{c(\rho)}{\rho}\right) > 0 \tag{15}$$

where $\nabla\lambda_{1,2}$ are the gradients of $\lambda_{1,2}$ with respect to ρ and v; prime denotes the differentiation with respect to ρ.

The homogeneous system (10) has two families of traffic sound waves, shock and rarefaction waves; one family for each characteristic field. For the first characteristic field, the properties of these waves are quantitatively identical to those of the LWR model because of $\lambda_1 \leqslant v$. But for the second characteristic field, the waves behave quite differently as they travel faster than traffic ($\lambda_2 \geqslant v$ and $\nabla\lambda_2(\rho, v)r_2(\rho, v) > 0$). This means that the future conditions of the traffic flow will be affected by the traffic conditions behind the flow. This type of behaviour, however, can be controlled by the factor β in our model. We call it the anisotropic factor. Note that $\beta \gg 1$, the second characteristic approaches v, the velocity of the traffic. Thus, information can never reach vehicles from behind. The term having this anisotropic factor in the system (9) is known as the anisotropic term.

2.3. Linear stability analysis

Assuming ρ_0 and $v_0 = \overline{V}(\rho_0)$ is the steady-state solution of equations (6) and (7). The analogous criterion for the continuum model may be found by linearizing the model around some initial values ρ_0 and v_0:

$$\rho = \rho_0 + \hat{\rho}. \tag{16}$$

$$v = v_0 + \hat{v}. \tag{17}$$

Taking Taylor series expansions of the perturbed equations at ρ_0 and v_0 leads to the perturbation equations

$$\frac{\partial\hat{\rho}}{\partial t} + \rho_0\frac{\partial\hat{v}}{\partial x} + v_0\frac{\partial\hat{\rho}}{\partial x} = 0, \tag{18}$$

and

$$\frac{\partial\hat{v}}{\partial t} + v_0\frac{\partial\hat{v}}{\partial x} = a[\overline{V}(\rho_0)\hat{\rho} - \hat{v}] + a\overline{V}'\left[\frac{1}{2\rho_0}\frac{\partial\hat{\rho}}{\partial x} + \frac{1}{6\rho_0^2}\frac{\partial^2\hat{\rho}}{\partial x^2}\right] - 2\beta c_0\frac{\partial\hat{v}}{\partial x}, \tag{19}$$

where $c_0 = c(\rho_0)$ and $\overline{V}' = \overline{V}'(\rho_0)$.

The linear stability of the system (9) can be determined by examining the sinusoidal solution of the perturbed equations (16) and (17). It is found that the system is stable when

$$\rho_0^2 - \frac{2\beta c_0 \rho_0}{\overline{V}'} < -\left(\frac{a(1+\beta^2)}{2\overline{V}'}\right). \tag{20}$$

The proof of the linear stability analysis can be found in appendix A of this paper. This shows that the model is stable against all infinitesimal perturbations for inequality (20). There is an intermediate range of density, $0 \leqslant \rho_{c_1} \leqslant \rho \leqslant \rho_{c_2}$, in which $\overline{V}(\rho)$ is so sensitive to change in ρ that homogeneous flow is unstable. As follows from inequality (20), one can find the critical values (ρ_{c_1} and ρ_{c_2}) from the equation

$$\rho_0^2 - \frac{2\beta c_0 \rho_0}{\overline{V}'} = -\left(\frac{a(1+\beta^2)}{2\overline{V}'}\right). \tag{21}$$

Note that for $\beta = 0$ we get

$$-\left(\frac{a}{2\rho_0^2 \overline{V}'}\right) > 1 \tag{22}$$

which is exactly the stability criterion found by Berg *et al* [15].

Due to the presence of anisotropic parameter, the intermediate range of instability in our model is different from Berg's model [15]. This explains the basic difference between these two models. These results are crucial in explaining the appearance of a 'phantom traffic jam', which is observed in a real traffic flow. In this regime, the traffic flow breaks down and forms the well-known stop-and-go pattern of a traffic jam [24].

It is easy to find out that the critical disturbances travel with a speed

$$\overline{C}(\rho_0) = \overline{V}(\rho_0) + \overline{V}'(\rho_0)\left(\rho_0 + \frac{a\beta}{2c_0}\right), \tag{23}$$

which is slower than the steady-state traffic speed $v_0 = \overline{V}(\rho_0)$, since $\overline{V}'$ is negative.

3. Travelling wave and shock

In this section, we study whether the new model smoothes out the shock waves of the LWR model. Now we examine the travelling waves in traffic flow. A travelling wave is a stable monotone and smooth wave from $(\rho, v)(x - Ut)$ that travels at a constant speed U and connects two constant states (ρ, v) $(\pm\infty)$.

Suppose that the new model admits a smooth travelling wave solution (ρ, v) $(x - Ut)$:

$$\rho = \rho(X), \quad v = v(X), \quad X = x - Ut. \tag{24}$$

Substituting the steady profile solution into equations (6) and (7), we have

$$-U\frac{\partial \rho}{\partial x} + \frac{\partial (v\rho)}{\partial x} = 0 \tag{25}$$

$$T\left[(v + 2\beta c - U)\frac{\partial v}{\partial x} - a\overline{V}'\left(\frac{1}{2\rho}\frac{\partial \rho}{\partial x} + \frac{1}{6\rho^2}\frac{\partial^2 \rho}{\partial x^2}\right)\right] = \overline{V} - v. \tag{26}$$

Integrating (25) and reformulating, we get

$$v = U - \frac{A}{\rho}, \tag{27}$$

where A is a constant. Substituting (27) into (26), and multiplying ρ on both sides, we obtain

$$-T\left[(U-v)(U-(v+2\beta c))+\frac{a\overline{V}'}{2}\right]\frac{\partial\rho}{\partial x}-\left(\frac{a\overline{V}'}{6\rho}\right)\frac{\partial^2\rho}{\partial x^2}=q_e-U\rho+A, \tag{28}$$

where $q_e=\rho\overline{V}(\rho)$. To find the curves between ρ_1 at $X=-\infty$ and ρ_2 at $X=\infty$, we inserted $\frac{\partial\rho}{\partial x}=\frac{\partial^2\rho}{\partial x^2}=0$, into equation (28). So U and A must satisfy

$$q_e(\rho_1)-U\rho_1+A=q_e(\rho_2)-U\rho_2+A=0, \tag{29}$$

thus the speed of the travelling wave is given by

$$U=\frac{q_e(\rho_1)-q_e(\rho_2)}{\rho_1-\rho_2}. \tag{30}$$

Since $q_e(\rho)$ is a concave flow density function, there may only exist steady compression waves, which implies that $\rho_1<\rho_2$. This concave function also guarantees that the right-hand side of equation (28) is always positive [20, 25, 30]. Therefore, when $-T\big[(U-v)(U-(v+2\beta c))+\frac{a\overline{V}'}{2}\big]$ remain positive within (ρ_1,ρ_2), then $\frac{\partial\rho}{\partial x}>0$ as the coefficient of $\frac{\partial^2\rho}{\partial x^2}$ is very small in comparison to the coefficient of $\frac{\partial\rho}{\partial x}$ and we have a smooth travelling wave solution.

For

$$-T\left[(U-v)(U-(v+2\beta c))+\frac{a\overline{V}'}{2}\right]>0, \tag{31}$$

we have

$$v+\beta c-\big(\sqrt{\beta^2+1}\big)c<U<v+\beta c+\big(\sqrt{\beta^2+1}\big)c. \tag{32}$$

When condition (31) is not satisfied or the right-hand side of equation (28) changes its sign at $\rho^*\in(\rho_1,\rho_2)$ then $\frac{\partial\rho}{\partial x}$ becomes infinity at that point (ρ^*) and the wave profile turns back. Since a single-valued continuous profile is no longer possible in this case, the analytical solution does not have any physical meaning and it should be replaced by a weak solution consisting of a discontinuity (i.e., a shock) [25, 30].

4. Numerical method

In this section, we review the numerical solution method. The following difference equations are obtained by applying the finite difference method on the system of equations (6) and (7):

$$\rho_i^{j+1}=\rho_i^j+\frac{\Delta t}{\Delta x}\rho_i^j\big(v_i^j-v_i^{j+1}\big)+\frac{\Delta t}{\Delta x}v_i^j\big(\rho_{i-1}^j-\rho_i^j\big), \tag{33}$$

(a) For heavy traffic (i.e. $v_i^j<-2\beta c(\rho)$)

$$\begin{aligned}v_i^{j+1}=v_i^j&+\frac{\Delta t}{\Delta x}\big(-2\beta c(\rho)-v_i^j\big)\big(v_{i+1}^j-v_i^j\big)-\frac{\Delta t}{T}\big(v_i^j-\overline{V}\big)\\&+\frac{\Delta t}{T}\overline{V}'\left[\frac{\big(\rho_{i-1}^j-\rho_i^j\big)}{2\Delta x\rho_i^j}+\frac{\big(\rho_{i-1}^j-2\rho_i^j+\rho_{i+1}^j\big)}{6(\Delta x)^2\big(\rho_i^j\big)^2}\right].\end{aligned} \tag{34}$$

(b) For light traffic (i.e. $v_i^j \geqslant -2\beta c(\rho)$)

$$v_i^{j+1} = v_i^j + \frac{\Delta t}{\Delta x}\left(-2\beta c(\rho) - v_i^j\right)\left(v_i^j - v_{i-1}^j\right) - \frac{\Delta t}{T}\left(v_i^j - \overline{V}\right) + \frac{\Delta t}{T}\overline{V}'\left[\frac{\left(\rho_{i-1}^j - \rho_i^j\right)}{2\Delta x \rho_i^j} + \frac{\left(\rho_{i-1}^j - 2\rho_i^j + \rho_{i+1}^j\right)}{6(\Delta x)^2\left(\rho_i^j\right)^2}\right] \tag{35}$$

where i and j represent the road section and time respectively.

The above difference scheme is suitable for the traffic flow as it maintains the physical properties of the traffic flow even under extreme conditions. For example, let us consider that at any time t_1, the density of any section x_1 is zero, i.e. $\rho_{x_1}^{t_1} = 0$, then we have

$$\frac{\partial \rho_{x_1}^{t_1}}{\partial t} = \frac{1}{\Delta x}\left[\rho_{x_1-1}^{t_1} v_{x_1}^{t_1} - \rho_{x_1}^{t_1} v_{x_1+1}^{t_1}\right]. \tag{36}$$

Since $\rho_{x_1}^{t_1} = 0$ and $\rho_{x_1-1}^{t_1} v_{x_1}^{t_1} \geqslant 0$, we get

$$\frac{\partial \rho_{x_1}^{t_1}}{\partial t} \geqslant 0. \tag{37}$$

This implies that the density will never be negative after the time t_1. On the other hand, let us assume that at any time t_1, the density of any section is maximum, i.e. $\rho_{x_1}^{t_1} = \rho_m$, then we have

$$v_{x_1}^{t_1} = 0 \quad \text{(as } \rho_m \text{ is the jam density)}. \tag{38}$$

Since $\rho_{x_1-1}^{t_1} v_{x_1}^{t_1} = 0$ and $\rho_{x_1}^{t_1} v_{x_1+1}^{t_1} \geqslant 0$, we get

$$\frac{\partial \rho_{x_1}^{t_1}}{\partial t} \leqslant 0, \tag{39}$$

which implies that density cannot exceed the maximum density. We can apply similar types of analyses also for the speed.

5. Shock and rarefaction waves

As already pointed out by Daganzo [18], the shock and rarefaction waves are the important traffic flow conditions and the realistic description of shock fronts in traffic is a particularly difficult problem. We have carried out numerical tests for two different values of anisotropic parameter to investigate whether our model can describe these important traffic conditions. Let us consider the two Riemann initial conditions, one describing congested upstream and nearly free downstream and vice versa. These two conditions are

$$\rho_u^1 = 0.04 \text{ veh m}^{-1} \qquad \rho_d^1 = 0.18 \text{ veh m}^{-1}, \tag{40}$$

$$\rho_u^2 = 0.18 \text{ veh m}^{-1} \qquad \rho_d^2 = 0.04 \text{ veh m}^{-1}, \tag{41}$$

where ρ_u and ρ_d are upstream and downstream densities, respectively. These situations are the realistic situations in traffic flow and can be described as follows: condition (40) corresponds to a situation where a nearly free-flow traffic meets a queue of nearly stopping vehicles, i.e. a shock wave situation, while condition (41) is just opposite to condition (40) and described as a rarefaction wave situation.

For initial condition, we take

$$v_u^{1,2} = \overline{V}\left(\rho_u^{1,2}\right), \qquad v_d^{1,2} = \overline{V}\left(\rho_d^{1,2}\right) \tag{42}$$

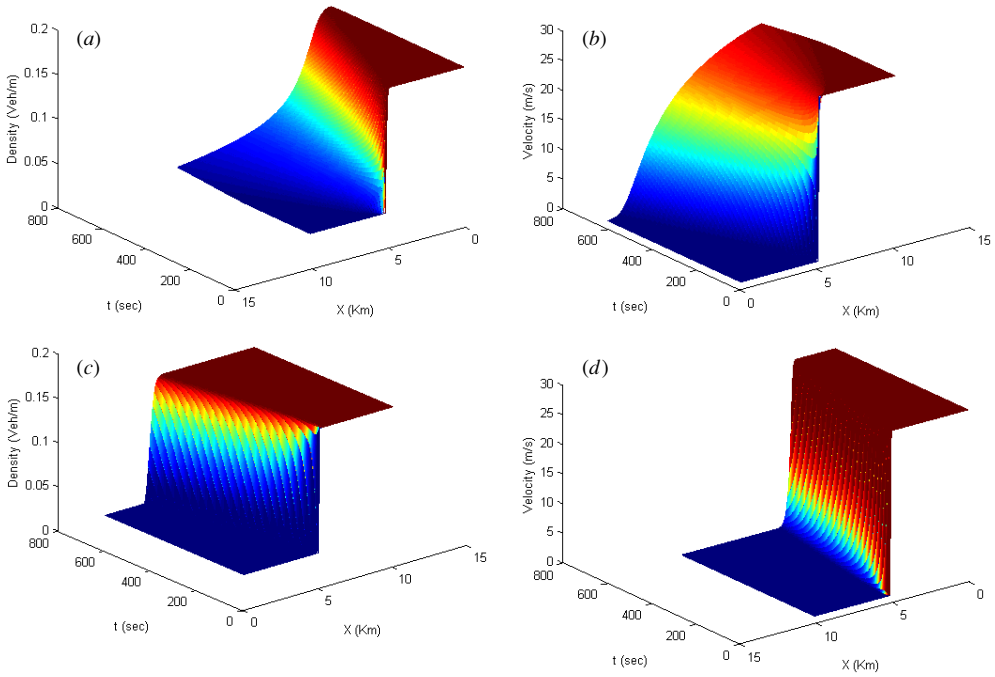

Figure 1. Shock and rarefaction waves under Riemann initial conditions (32) and (33) for $\beta = 3$: (*a*) and (*c*) temporal development of density $\rho(x, t)$; (*b*) and (*d*) temporal development of speed $v(x, t)$. In (*a*) and (*d*), the direction of the space axis is reversed for illustrative purposes.

where $\overline{V}(\rho) = v_f\left[1 - \exp\left(1 - \exp\left(\frac{c_m}{v_f}\left(\frac{\rho_m}{\rho} - 1\right)\right)\right)\right]$ is the equilibrium speed–density relationship, which is developed by Del Castillo *et al* [31]. Here v_f is the free-flow speed, ρ_m is the maximum or jam density and c_m is the kinematic wave speed under jam density.

We have taken the test road section as 20 km long and for numerical calculations it is divided into 100 meshes of equal length. The related parameters of our model are as follows:

$$v_f = 30 \text{ m s}^{-1}, \quad \rho_m = 0.2 \text{ veh m}^{-1}, \quad T = 10 \text{ s} \quad \text{and} \quad c_m = 11 \text{ m s}^{-1}. \tag{43}$$

Figures 1 and 2 depict the wave that develops from the Riemann initial conditions (40) and (41) for two different values of anisotropic parameter β. It is clear from the figures 1 and 2 that the new model provides correct predictions under the two Riemann initial conditions.

Taking $\beta = 3$, we substitute the values into equations (30) and (32), and find out that inequality (32) is not satisfied under the initial condition (40), which means that there should be a shock under the given condition and the propagation speed of the shock is found to be negative from equation (30). Figures 1(*a*) and (*b*) show how the backward moving shock wave front evolves and figures 1(*c*) and (*d*) describe how the rarefaction wave front evolves. It is clear from figures 1(*a*) and (*b*) that the moving front is smoothed over time. Such types of results are also found out by Jiang *et al* [25]. But figures 1(*c*) and (*d*) cannot describe the real traffic situation because the discontinuity cannot move with the initial shape as defined by Berg *et al* [15]. To overcome this difficulty, we increase the value of β for $\beta = 20$, the graph of velocity and density profile under the initial conditions (40) and (41) is given in figure 2, which shows the consistency of our model with the real traffic flow. Hence the parameter β plays a crucial role in making our model realistic.

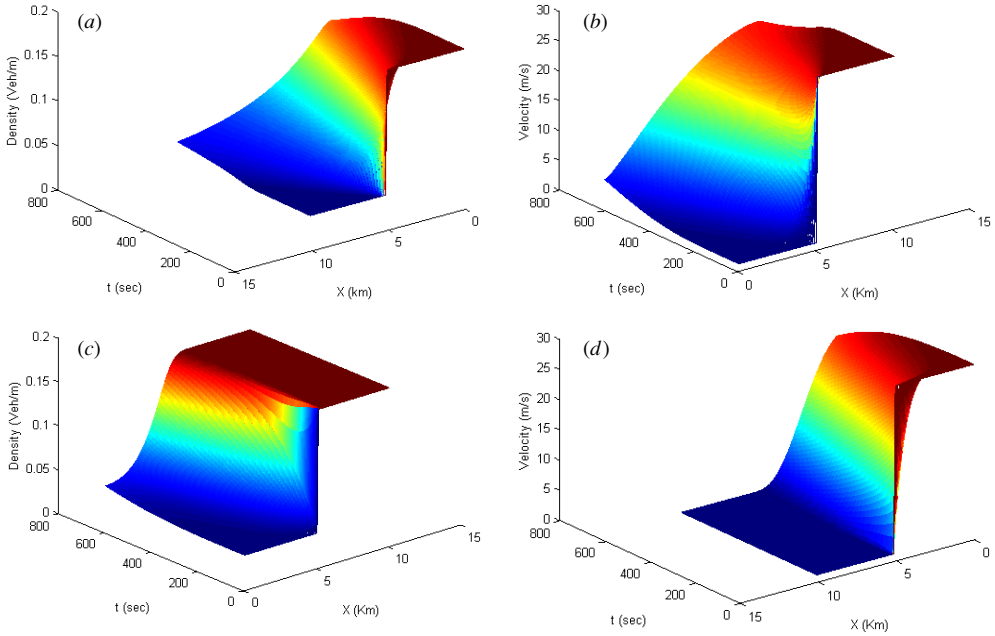

Figure 2. Shock and rarefaction waves under Riemann initial conditions (32) and (33) for $\beta = 20$: (*a*) and (*c*) temporal development of density $\rho(x, t)$; (*b*) and (*d*) temporal development of speed $v(x, t)$. In (*a*) and (*d*), the direction of the space axis is reversed for illustrative purposes.

6. Local cluster effect

The new anisotropic model can also describe the nonlinear theory of the cluster effect in a traffic flow, i.e., the effect of the appearance of a region of high density and low average velocity of vehicles in an initially homogeneous flow. To investigate the local cluster effect, we apply the numerical scheme given in section 4. Let us consider the behaviour of a localized perturbation, which at time $t = 0$, occurs in an initial homogeneous state of traffic flow and is given by

$$\rho(x, 0) = \rho_h + \Delta\rho(x) \qquad x \in [0, L] \tag{44}$$

$$v(x, 0) = \overline{V}(\rho(x, 0)) \qquad x \in [0, L]. \tag{45}$$

For numerical investigation, the following shape of the localized perturbation is used as in [24]

$$\Delta\rho(x) = \Delta\rho_0 \left\{ \cosh^{-2}\left(\frac{160}{L}\left(x - \frac{5L}{16}\right)\right) - \frac{1}{4}\cosh^{-2}\left(\frac{40}{L}\left(x - \frac{11L}{32}\right)\right)\right\}, \tag{46}$$

where L is the length of road section under consideration. The periodic boundary condition for the simulation to describe the amplification of small disturbances is given by

$$\rho(L, t) = \rho(0, t), \qquad v(L, t) = v(0, t). \tag{47}$$

For equilibrium speed–density relationship, we use the following relation proposed by Kerner and Konhäuser [11]:

$$\overline{V}(\rho) = u_f \left[\left(1 + \exp\left(\frac{\frac{\rho}{\rho_m} - 0.25}{0.06}\right)\right)^{-1} - 3.72 \times 10^{-6}\right]. \tag{48}$$

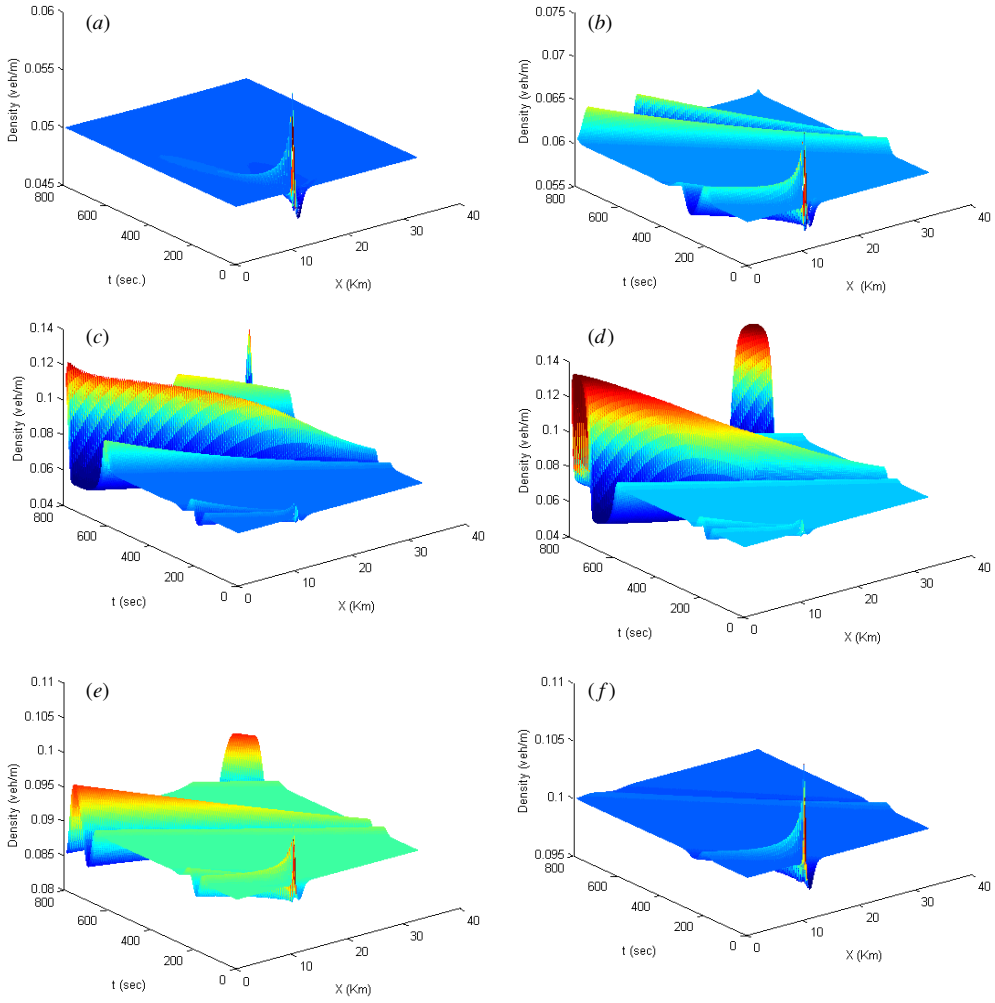

Figure 3. Temporal evolution of traffic density on a ring road of circumference 32.2 km with a homogeneous initial traffic under condition (41) and a localized perturbation of amplitude $\Delta\rho_0 = 0.01$ veh m^{-1} for (*a*) $\rho_h = 0.05$ veh m^{-1}; (*b*) $\rho_h = 0.06$ veh m^{-1}; (*c*) $\rho_h = 0.07$ veh m^{-1}; (*d*) $\rho_h = 0.08$ veh m^{-1}; (*e*) $\rho_h = 0.09$ veh m^{-1}; (*f*) $\rho_h = 0.1$ veh m^{-1}.

For computational purpose, the space domain is divided into equal intervals of length 200 m and time interval is chosen as 1 s.

We take two different sets of parameter to show that our model can also describe the local cluster effect of traffic flow [11, 21, 24]:

$$\beta = 6.0, \quad u_f = 125 \text{ m s}^{-1}, \quad T = 14 \text{ s} \quad \text{and} \quad \rho_m = 0.25 \text{ veh m}^{-1} \tag{49}$$

$$\beta = 20.0, \quad u_f = 170 \text{ m s}^{-1}, \quad T = 25 \text{ s} \quad \text{and} \quad \rho_m = 0.9 \text{ veh m}^{-1}. \tag{50}$$

The critical values corresponding to the parameters (49) and (50) are 0.060 367, 0.092 182 and 0.250 102, 0.292 249, respectively, which can easily be found out by substituting the parameter values into the stability condition (21). The traffic flow will be unstable between these critical densities. Taking different values of initial density for both sets of parameters,

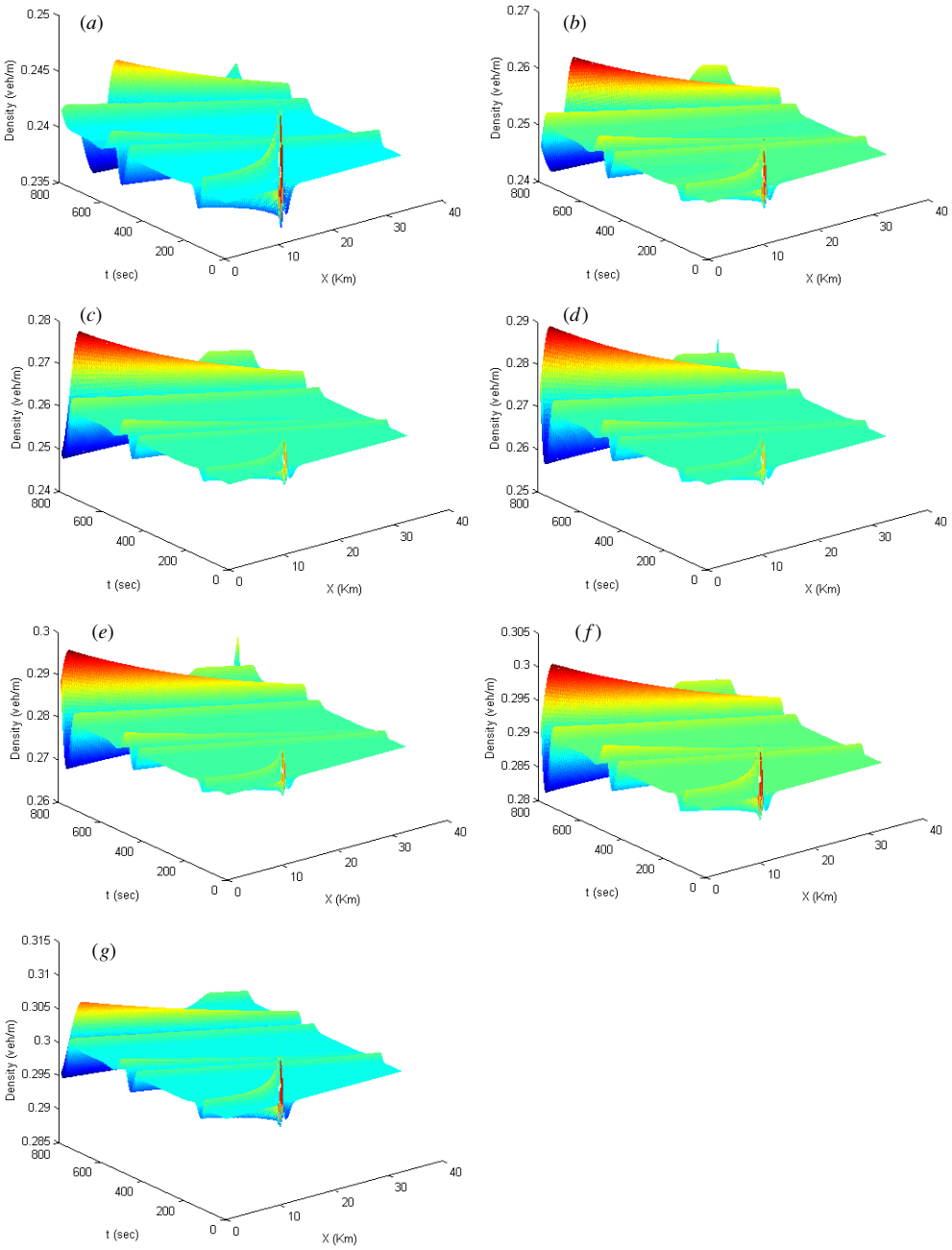

Figure 4. Temporal evolution of traffic density on a ring road of circumference 32.2 km with a homogeneous initial traffic under condition (42) and a localized perturbation of amplitude $\Delta\rho_0 = 0.01$ veh m^{-1} for (*a*) $\rho_h = 0.24$ veh m^{-1}; (*b*) $\rho_h = 0.25$ veh m^{-1}; (*c*) $\rho_h = 0.26$ veh m^{-1}; (*d*) $\rho_h = 0.27$ veh m^{-1}; (*e*) $\rho_h = 0.28$ veh m^{-1}; (*f*) $\rho_h = 0.29$ veh m^{-1}; (*g*) $\rho_h = 0.3$ veh m^{-1}.

we investigate the traffic density pattern with respect to time and results for two different values of β are shown in figures 3 and 4.

In figure 3(a), the traffic flow density is very low and the perturbation dies out with time, which shows a good agreement with the Herrman and Kerner theory [24] that below the critical density, the initially homogeneous state of traffic flow is stable with respect to the growth of any non-homogeneous perturbations with small enough amplitudes. As the initial density increases, the amplitude of the initial small perturbations grows in time. Figure 3(b) shows that when the initial density is just above the down critical density a complex localized structure of two clusters forms. This situation corresponds to stop-and-go traffic. Further increase in initial density leads to a dipole-like structure as illustrated by figures 3(c) and (d). In figure 3(d) the density of the cluster increases more rapidly than in figure 3(c). It is clear from figure 3(e) that the non-homogeneous perturbations are slowly amplified when the initial density is nearer to the up critical density. Finally, when the density becomes greater than the up critical density, a stable regime is reached again as can be seen in figure 3(f).

Similarly, figure 4 describes the growth of the localized perturbation for different values of initial density with the parameters given in equation (50). The results are found to be the same as results for the parameter values in (49) and shown graphically by figures 3(a)–(f). It is observed that for $\beta = 20$, the shape of the cluster for different initial data is the same. Figure 4 illustrates that with the growth of the small amplitude perturbations, a non-stationary cluster forms. Firstly, the perturbation decreases and as time increases the amplitude of the perturbation increases. The cluster of vehicles represents a locally moving region, where the density is higher and the average velocity is lower than the initial flow and outside the cluster.

Therefore for both the values of anisotropic parameter, the above results show a good agreement with the results found by Kerner and Konhäuser [11, 21], Herrman and Kerner [24], Jiang *et al* [25] and Treiber *et al* [32].

7. Conclusion

In traffic flow, in spite of its simplicity the LWR model is a remarkably robust and powerful theory, but it is unable to describe the important traffic phenomena, such as vehicle clustering. In the literature of macroscopic traffic theory, especially that of higher order models, the research on the shock and rarefaction waves and the cluster effect has an important significance. In this paper, we investigated numerically the shock and rarefaction waves together with the vehicle clustering in the anisotropic continuum model. We presented a simple finite difference scheme to carry out the numerical simulation and discuss the applicability of the scheme in some special cases. Travelling and shock wave solutions are given in section 3. To discuss the performance of the model, we take two different values of the anisotropic parameter. Finally, the numerical tests verify that the model is able to simulate complex traffic phenomena observed in traffic flow, such as shock waves, rarefaction waves and local cluster effects. Comparing the numerical results with those presented by Jiang *et al* [25], Kerner and Konhäuser [11, 21], we find that the clusters have almost the same structure for different values of the anisotropic parameter. Our model is analogous to the Kerner–Konhäuser model [11]. However, an important difference between Kerner–Konhäuser model and the new model lies in the coefficient of the higher order terms. In Kerner–Konhäuser model, the coefficients are assumed to be constant but in our model they actually depend on density (ρ). This clarifies that the analysis of the new model is an improvement over the higher order models presented in the literature.

Further investigations need to be carried out to test the performance of the new anisotropic continuum model in modelling real traffic. So it may be reasonable to conclude that the new model provides a more accurate description of traffic flow and results obtained are consistent with the spectrum of nonlinear dynamic properties reported in the literature.

Acknowledgments

The authors are grateful to the anonymous referees for their suggestions to improve the paper. This work is supported by the Junior Research Fellowship to one of the authors (AK) from Council of Scientific and Industrial Research (CSIR), New Delhi, India.

Appendix

To determine the stability condition of the system (9), we calculate the eigenvalue $\omega(k)$ of a harmonic disturbance

$$\overline{f}(x,t) = \begin{pmatrix} \hat{\rho}(x,t) \\ \hat{v}(x,t) \end{pmatrix} = \begin{pmatrix} \hat{\rho}_0 \\ \hat{v}_0 \end{pmatrix} \exp\{\mathrm{i}[kx - \omega(k)t]\}, \tag{A1}$$

so that we can rewrite equations (18) and (19) in the form

$$\begin{pmatrix} \mathrm{i}(kv_0 - \omega) & \mathrm{i}k\rho_0 \\ -a\overline{V}' - \frac{a\mathrm{i}k\overline{V}'}{2\rho_0} + \frac{a\overline{V}'k^2}{6\rho_0^2} & \mathrm{i}(kv_0 - \omega) + a + 2\beta c_0 \mathrm{i}k \end{pmatrix} \begin{pmatrix} \hat{\rho}_0 \\ \hat{v}_0 \end{pmatrix} \exp\{\mathrm{i}[kx - \omega(k)t]\} = 0, \tag{A2}$$

for nontrivial solution

$$\begin{vmatrix} \mathrm{i}(kv_0 - \omega) & \mathrm{i}k\rho_0 \\ -a\overline{V}' - \frac{a\mathrm{i}k\overline{V}'}{2\rho_0} + \frac{a\overline{V}'k^2}{6\rho_0^2} & \mathrm{i}(kv_0 - \omega) + a + 2\beta c_0 \mathrm{i}k \end{vmatrix} = 0. \tag{A3}$$

On solving this, we get

$$\omega_{1,2}(k) = k(v_0 + \beta c_0) - \frac{a\mathrm{i}}{2}\left[1 \pm \sqrt{1 + \frac{2\overline{V}'}{a}\left(k^2(\beta^2+1) - \frac{a\mathrm{i}\beta k}{c_0} - 2\mathrm{i}k\rho_0 + \frac{\mathrm{i}k^3}{3\rho_0}\right)}\right]. \tag{A4}$$

The traffic flow will remain stable as long as the imaginary part of ω is negative.

Define

$$\Omega(k) = \mathrm{Re}\left[1 + \frac{2\overline{V}'}{a}\left(k^2(\beta^2+1) - \frac{a\mathrm{i}\beta k}{c_0} - 2\mathrm{i}k\rho_0 + \frac{\mathrm{i}k^3}{3\rho_0}\right)\right]^{\frac{1}{2}}, \tag{A5}$$

the criterion is equivalent to $|\Omega(k)| < 1$, and

$$|\Omega(k)| = \left[\left(1 + \frac{2\overline{V}'}{a}k^2(\beta^2+1)\right)^2 + \left(\frac{4\beta k c_0}{a} - \frac{4k\rho_0\overline{V}'}{a} + \frac{2k^3\overline{V}'}{3a\rho_0}\right)^2\right]^{\frac{1}{4}} \sqrt{\frac{1+\cos\phi}{2}}, \tag{A6}$$

where

$$\phi = \arg\left[1 + \frac{2\overline{V}'}{a}\left(k^2(\beta^2+1) - \frac{a\mathrm{i}\beta k}{c_0} - 2\mathrm{i}k\rho_0 + \frac{\mathrm{i}k^3}{3\rho_0}\right)\right]. \tag{A7}$$

Solving $|\Omega(k)| = 1$ leads to three solutions

$$k_0 = 0, \qquad k_\pm = \sqrt{6\left(\rho_0^2 - \frac{\beta c_0\rho_0}{\overline{V}'}\right) \pm \frac{3a\rho_0}{\overline{V}'}\sqrt{\frac{-2\overline{V}'}{a}(1+2\beta^2)}}. \tag{A8}$$

We know that $\overline{V}' < 0$ and k_- is always real whereas k_+ might be either real or complex. As pointed out by Berg *et al* [15] the system is stable when $k_+ \notin R$, which means that

$$6\left(\rho_0^2 - \frac{\beta c_0\rho_0}{\overline{V}'}\right) + \frac{3a\rho_0}{\overline{V}'}\sqrt{\frac{-2\overline{V}'}{a}(1+2\beta^2)} < 0 \tag{A9}$$

or

$$\rho_0^2 - \frac{2\beta c_0\rho_0}{\overline{V}'} < -\left(\frac{a(1+\beta^2)}{2\overline{V}'}\right). \tag{A10}$$

References

[1] Fukui M, Sugiyama Y, Schreckenberg M and Wolf D E (ed) 2003 *Traffic and Granular Flow '01* (Berlin: Springer)
[2] Bellomo N, Delitala M and Coscia V 2002 *Math. Models Methods Appl. Sci.* **12** 1801–44
[3] Gerlough D L and Huber M J 1975 *Special Report no 165* (Washington, DC: Transportation Research Board, National Research Council)
[4] Helbing D 2001 *Rev. Mod. Phys.* **73** 1067–144
[5] Lighthill M J and Whitham G B 1955 *Proc. R. Soc.* A **229** 317–45
[6] Richards P I 1956 Shock waves on the highway *Operations Research* **4** 42–51
[7] Prigogine I and Herman R 1971 (New York: Elsevier)
[8] Helbing D 1996 *Phys. Rev.* E **53** 2366
[9] Payne H J 1971 *Mathematical Models of Public Systems (Simulation Councils Proc. Ser.* vol 1*)* ed G A Bekey (La Jolla, CA: Simulation Councils Inc.) pp 51–60
[10] Phillips W F 1979 *Transp. Plan. Technol.* **5** 131–8
[11] Kerner B S and Konhäuser P 1993 *Phys. Rev.* E **48** 2335–8
[12] Zhang H M 1998 *Trans. Res.* B **32** 485–98
[13] Zhang H M 2003 *Trans. Res.* B **37** 27–41
[14] Zhang H M 2002 *Trans. Res.* B **36** 275–90
[15] Berg P, Mason A and Woods A 2000 *Phys. Rev.* E **61** 1056–66
[16] Zhang H M 2003 *Trans. Res.* B **37** 101–5
[17] Lax P D 1972 *Hyperbolic Systems of Conservation Laws and Mathematical Theory of Shock Waves* (Philadelphia, PA: Soc. Industrial and Applied Mathematics)
[18] Daganzo C F 1995 *Trans. Res.* B **29** 277–86
[19] Zhang H M 2000 *Trans. Res.* B **34** 583–603
[20] Whitham G B 1974 *Linear and Nonlinear Waves* (New York: Wiley)
[21] Kerner B S and Konhäuser P 1994 *Phys. Rev.* E **50** 54–83
[22] Coscia V 2004 *C. R. Mecanique* **332** 585–90
[23] Bürger R and Karlsen K H 2003 *Math. Models Methods Appl. Sci.* **13** 1767–99
[24] Herrmann M and Kerner B S 1998 *Physica* A **255** 163–88
[25] Jiang R, Wu Q and Zhu Z 2002 *Trans. Res.* B **36** 405–19
[26] Kerner B S 1998 *Phys. Rev. Lett.* **81** 3797–800
[27] Kerner B S 2002 *Math. Comput. Modelling* **35** 481–508
[28] Kerner B S and Rehborn H 1997 *Phys. Rev. Lett.* **79** 4030–3
[29] Zhou X, Liu Z and Luo J 2002 *J. Phys. A: Math. Gen.* **35** 4495–500
[30] Del Castillo J M, Pintado P and Benitez F G 1994 *Trans. Res.* B **28** 35–60
[31] Del Castillo J M and Benitez F G 1995 *Trans. Res.* B **29** 373–406
[32] Treiber M, Hennecke A and Helbing D 1999 *Phys. Rev.* E **59** 239–53